

Multi-gene phylogeny and divergence estimations for Evaniidae (Hymenoptera)

Barbara J Sharanowski¹, Leanne Peixoto², Anamaria Dal Molin³, Andrew R Deans^{Corresp.}⁴

¹ Department of Biology, University of Central Florida, Orlando, Florida, United States

² Department of Agroecology, Aarhus University, Aarhus, Denmark

³ Departamento de Ciências Biológicas, Universidade Federal do Espírito Santo, Vitória, ES, Brazil

⁴ Frost Entomological Museum, Department of Entomology, Pennsylvania State University, University Park, PA, United States

Corresponding Author: Andrew R Deans

Email address: adeans@psu.edu

Ensign wasps (Hymenoptera: Evaniidae) develop as predators of cockroach eggs (Blattodea), have a wide distribution and exhibit numerous interesting biological phenomena. The taxonomy of this lineage has been the subject of several recent, intensive efforts, but the lineage lacked a robust phylogeny. In this paper we present a new phylogeny, based on increased taxonomic sampling and data from six molecular markers (mitochondrial *16S* and *COI*, and nuclear markers *28S*, *RPS23*, *CAD*, and *AM2*), the latter used for the first time in phylogenetic reconstruction. Our intent is to provide a robust phylogeny that will stabilize and facilitate revision of the higher-level classification. We also show the continued utility of molecular motifs, especially the presence of an intron in the *RPS23* fragments of certain taxa, to diagnose evaniid clades and assist with taxonomic classification. Furthermore, we estimate divergence times among evaniid lineages for the first time, using multiple fossil calibrations. Evaniidae radiated primarily in the Early Cretaceous (134.1-141.1 Mya), with and most extant genera diverging near the K-T boundary. The estimated phylogeny reveals a more robust topology than previous efforts, with the recovery of more monophyletic taxa and better higher-level resolution. The results facilitate a change in ensign wasp taxonomy, with *Parevania*, **syn. nov.**, and *Papatuka*, **syn. nov.** becoming junior synonyms of *Zeuxevania*, and *Acanthinevania*, **syn. nov.** being designated as junior synonym of *Szepligetella*. We transfer 30 species to *Zeuxevania*, either reestablishing past combinations or as new combinations. We also transfer 20 species from *Acanthinevania* to *Szepligetella* as new combinations.

Multi-gene phylogeny and divergence time estimations for Evaniidae (Hymenoptera)

Barbara J. Sharanowski¹, Leanne Peixoto², Anamaria Dal Molin³, and Andrew R. Deans⁴

¹University of Central Florida, Department of Biology, 4110 Libra Drive, BIO 301, Orlando, Florida, USA 32816-2368

²Aarhus University, Department of Agroecology, Aarhus, Denmark, AU Foulum, Blichers Allé 20 8830 Tjele

³Depto. Ciências Biológicas, Universidade Federal do Espírito Santo, Vitória, ES, Brazil

⁴Frost Entomological Museum, Department of Entomology, 501 ASI Building, Pennsylvania State University, University Park, PA USA 16802

Corresponding author:

Andrew R. Deans⁴

Email address: adeans@psu.edu

ABSTRACT

Ensign wasps (Hymenoptera: Evaniidae) develop as predators of cockroach eggs (Blattodea), have a wide distribution and exhibit numerous interesting biological phenomena. The taxonomy of this lineage has been the subject of several recent, intensive efforts, but the lineage lacked a robust phylogeny. In this paper we present a new phylogeny, based on increased taxonomic sampling and data from six molecular markers (mitochondrial *16S* and *COI*, and nuclear markers *28S*, *RPS23*, *CAD*, and *AM2*), the latter used for the first time in phylogenetic reconstruction. Our intent is to provide a robust phylogeny that will stabilize and facilitate revision of the higher-level classification. We also show the continued utility of molecular motifs, especially the presence of an intron in the *RPS23* fragments of certain taxa, to diagnose evaniid clades and assist with taxonomic classification. Furthermore, we estimate divergence times among evaniid lineages for the first time, using multiple fossil calibrations. Evaniidae radiated primarily in the Early Cretaceous (134.1–141.1 Mya), with and most extant genera diverging near the K-T boundary. The estimated phylogeny reveals a more robust topology than previous efforts, with the recovery of more monophyletic taxa and better higher-level resolution. The results facilitate a change in ensign wasp taxonomy, with *Parevania*, **syn. nov.**, and *Papatuka*, **syn. nov.** becoming junior synonyms of *Zeuxevania*, and *Acanthinevania*, **syn. nov.** being designated as junior synonym of *Szepligetella*. We transfer 30 species to *Zeuxevania*, either reestablishing past combinations or as new combinations. We also transfer 20 species from *Acanthinevania* to *Szepligetella* as new combinations.

INTRODUCTION

Ensign wasps (Hymenoptera: Evaniidae) are common, nearly cosmopolitan, and include approximately 500 extant species in 21 genera, although many species remain to be described (Deans, 2005). Their biology lies at the precipice between wasps that provision their young with prey and parasitic wasps that deposit their offspring to feed on one host. A female evaniid wasp lays a single egg within a cockroach egg case and their offspring feeds on the unhatched cockroach eggs. Because their larvae feed on multiple hosts, ensign wasps are regarded as predators as opposed to parasitoids (Huben, 1995). However, the intimate association that larval evaniids have with their prey is much more reminiscent of parasitoid behavior. Despite these interesting biological features, there is scant research aimed at understanding their evolution and natural history. This predicament remains, in part, due to ongoing instability in their classification and the lack of robust diagnostic tools and inadequate taxon descriptions. Taxonomic work over the last 20 years, however, including a key to genera (Deans and Huben, 2003), a comprehensive species catalog (Deans, 2005, treating all ca. 500 species), descriptions of fossils (Deans et al., 2004; Jennings et al., 2013, 2012, 2004), and updated (Deans and Kawada, 2008) and semantically-enhanced

47 species-level revisions (Balhoff et al., 2013; Mikó et al., 2014) have substantially increased the potential
48 for research on these insects.

49 Deans et al. (2006) also published the first phylogeny of the family, which was an attempt to test the
50 historic generic and tribal classifications. Of the 17 included genera, four were represented by single
51 specimens: *Papatuka* Deans, *Rothevania* Huben (monotypic), *Thaumatevania* Ceballos (monotypic),
52 and *Trissevania* Kieffer. Six genera were found to be monophyletic in both a parsimony and Bayesian
53 analysis, including: *Acanthinevania* Bradley, *Decevania* Huben, *Evania* Fabricius, *Evaniscus* Szépligeti,
54 *Micrevania* Benoit, and *Semaemyia* Bradley. Although *Prosevania* Kieffer was always recovered,
55 with one possibly misplaced specimen of *Szepligetella* Bradley, it is likely that *Prosevania* may also
56 be monophyletic. Several other genera were consistently recovered as paraphyletic or in unresolved
57 polytomies, including *Brachygaster* Leach, *Evaniella* Bradley, *Hyptia* Illiger, *Szepligetella* Bradley,
58 *Parevania* Kieffer, and *Zeuxevania* Kieffer. The latter two genera were consistently recovered in a clade
59 with *Papatuka* Deans, and Deans et al. (2006) suggested that these taxa may be congeneric based on
60 the molecular results and inconsistencies in the morphological character that separates these two genera
61 (presence of fore wing 1RS in *Parevania*). They also suggested *Evaniella* may be monophyletic as it
62 was consistently recovered with the exception of one aberrant taxon, since described as its own genus
63 (*Alobevania* Deans and Kawada, 2008)).

64 The only tribal classification put forth for Evaniidae was by Bradley (1908), who suggested two
65 tribes for the ten genera described at the time: Hyptiini (including *Evaniella*, *Evaniscus*, *Hyptia*, *Pare-*
66 *vania*, *Semaemyia*, and *Zeuxevania*) and Evaniini (including *Acanthinevania*, *Evania*, *Prosevania*, and
67 *Szepligetella*). This tribal classification was not supported by Deans et al. (2006). There was not enough
68 resolution to confidently resolve relationships among evaniid genera to develop a better tribal classification.
69 Deans et al. (2006) did suggest that the New World taxa with reduced wing venation (including *Evaniscus*,
70 *Decevania*, *Hyptia*, *Rothevania*, and *Semaemyia*) were monophyletic and could represent a tribe.

71 The poorly resolved phylogenies published by Deans et al. (2006) may be attributed to low taxonomic
72 sampling, as only 54 ingroup taxa were included, or, more likely, a lack of informative sites in the sequence
73 data. The resulting “backbone polytomy”, where higher-level classifications remain elusive, is common in
74 other phylogenies of Hymenoptera that use the same or similar sets of genes (Dowton and Austin, 2001;
75 Mardulyn and Whitfield, 1999; Pitz et al., 2007). Divergence times for members of Evaniidae have not
76 been estimated before. Several recent studies on Hymenoptera have estimated stem-age divergences for
77 Evanioidea ranging from 175 Ma to 221 Ma (Ronquist et al., 2012a; Zhang et al., 2015; Peters et al.,
78 2017; Branstetter et al., 2017). Unfortunately, the small sample size for Evanioidea in all of these studies
79 (1–3 exemplars) and uncertainty in phylogenetic relationships of Evanioidea within Hymenoptera resulted
80 in wide confidence intervals around the estimates. Based on all fossils placed within Evanioidea, it is
81 likely that the superfamily diversified in the Middle Jurassic but may have originated as early as the late
82 Triassic (Li et al., 2018).

83 Here we attempt to gain a better understanding of higher-level relationships among genera and better
84 test the monophyly of genera, using an increased taxonomic and genetic sampling dataset, including
85 a handful of new protein-coding genes. Our intent is to provide a robust phylogeny that will stabilize
86 and facilitate revision of the higher-level classification. We also show the continued utility of molecular
87 motifs, first described for Evaniidae by Deans et al. (2006), to diagnose clades and assist with taxonomic
88 classification. Furthermore, we estimate divergence times among evaniid lineages for the first time, using
89 multiple fossil calibrations to understand of the timing of diversification in Evaniidae.

90 MATERIALS AND METHODS

91 Taxon sampling

92 A list of taxa and sequences utilized in this study is presented in Table 1 (more details in Table S1).
93 Exemplars were obtained for 89 evaniid specimens, across 17 genera, and five outgroup taxa, including
94 two species of *Gasteruption* (Gasteruptionidae) and three species of *Pristaulacus* (Aulacidae), for a total
95 of 94 taxa. All evaniid genera were represented except four rare genera: *Afrevania*, *Brachevania*,
96 *Thaumatevania*, and *Vernevania*. We were only able to include one representative of *Alobevania* and
97 *Rothevania* (monotypic), and *Papatuka*. Where possible, sampling was increased for genera that were
98 previously recovered as paraphyletic by Deans et al. (2006).

taxon	Ext.	DV#	28S	AM2	CAD1	CAD2	RPS23	COI	16S
<i>Gasteruption</i> 300	300		X		X	X	X	X	D
<i>Gasteruption</i> 244	244		X		X		X	X	
<i>Pristaulacus strangaliae</i>	176			X			X	X	
<i>Pristaulacus fasciatus</i>	299							X	
<i>Pristaulacus</i> 21	306	21	D				X	D	D
<i>Acanthinevania</i> 240	240		X	X	X	X	X	X	
<i>Acanthinevania</i> 242	242		X	X	X	X	X		
<i>Acanthinevania princeps</i>	246		X		X	X	X	X	
<i>Acanthinevania</i> 001	271	001	D	X	X	X	X	D	D
<i>Acanthinevania</i> 033	289	033	D	X	X	X	X	D	D
<i>Acanthinevania</i> 049	292	049	D	X	X	X	X	D	D
<i>Alobevania gattiae</i>	200	039	D	X	X	X		X	D
<i>Brachygaster minutus</i>	273	030	X		X	X	X	D	D
<i>Brachygaster minutus</i>	512				X	X		X	
<i>Brachygaster</i> 037	286		D		X		X		D
<i>Brachygaster</i> 050	290		D				X		D
<i>Decevania</i> 502	502				X	X			
<i>Decevania</i> 513	513			X				X	
<i>Decevania</i> 004	274	004	D	X		X	X	D	D
<i>Decevania</i> 005	301	005	D				X		D
<i>Decevania</i> 063	296	063	D	X	X	X	X	D	D
<i>Evania</i> 175	175		X				X	X	
<i>Evania albofacialis</i>	275	020	D		X	X	X	D	D
<i>Evania appendigaster</i>	207	046	D		X	X	X	D	D
<i>Evania</i> 496	496		X			X	X	X	
<i>Evania</i> 002	189	002	D		X	X		D	D
<i>Evaniella</i> 230	230		X	X	X	X	X	X	
<i>Evaniella</i> 234	234		X	X		X	X	X	
<i>Evaniella</i> 237	237			X	X			X	
<i>Evaniella</i> 485	485			X	X	X	X		
<i>Evaniella</i> 486	486			X	X		X		
<i>Evaniella</i> 493	493				X		X	X	
<i>Evaniella semaeoda</i>	220	058	D				X	D	D
<i>Evaniella</i> 019	192	019	D	X	X		X	D	
<i>Evaniella</i> 025	307	025	D		X		X	D	D
<i>Evaniella</i> 045	206	045	D	X	X		X		D
<i>Evaniscus marginatus</i>	213	052	D				X		D
<i>Evaniscus rufithorax</i>	206		D			X	X	X	D
<i>Hyptia</i> 232	232			X	X	X	X	X	
<i>Hyptia</i> 487	487			X				X	
<i>Hyptia</i> 501	501			X	X			X	
<i>Hyptia</i> 511	511			X	X			X	
<i>Hyptia amazonica</i>	235				X	X		X	
<i>Hyptia floridana</i>	291	009	D	X	X	X		D	D
<i>Hyptia</i> 007	302	007	D		X		X	D	D
<i>Hyptia</i> 008	303	008	D				X	D	D
<i>Micrevania difficilis</i>	283	006	D		X	X		X	D
<i>Micrevania</i> 061	288	061	D	X		X		D	D
<i>Micrevania</i> 066	298	066	D			X		D	D
<i>Micrevania</i> 026	308	026	D			D		D	D
<i>Papatuka capensis</i>	227	065	D		X	X	X	X	D
<i>Parevania</i> 172	172		X	X	X		X		
<i>Parevania</i> 174	174		X	X			X	X	

Continued on next page

Table 1 – Continued from previous page

taxon	Ext.	DV#	28S	AM2	CAD1	CAD2	RPS23	COI	16S
<i>Parevania</i> 041	295	041	D	X	X	X	X	D	D
<i>Parevania</i> 057	219	057	D	X	X	X	X		D
<i>Parevania</i> 064	276	064	D		X	X	X	D	D
<i>Prosevania fuscipes</i>	224	062	D			X		X	D
<i>Prosevania</i> 497	497		X	X	X	X		X	
<i>Prosevania</i> 498	498				X			X	
<i>Prosevania</i> 508	508							X	
<i>Prosevania</i> 027	309	027	D	X		X		X	D
<i>Prosevania</i> 034	277	034	D					D	D
<i>Prosevania</i> 036	284	036	D		X	X		X	D
<i>Prosevania</i> 044	205	044	D	X	X	X	X	D	D
<i>Rothevania valdivianus</i>	239	048	D	X	X	X		D	D
<i>Semaeomyia</i> 489	489				X	X	X	X	
<i>Semaeomyia</i> 509	509		X			X	X	X	
<i>Semaeomyia</i> 510	510		X			X	X	X	
<i>Semaeomyia leucomelas</i>	305	016	D			X	X	D	D
<i>Semaeomyia</i> 012	197	012	D		X	X		D	D
<i>Semaeomyia</i> 051	279	051	D			X	X	D	D
<i>Semaeomyia</i> 059	293	059	D	X		X	X	D	D
<i>Szepligetella</i> 170	170				X		X	X	
<i>Szepligetella</i> 231	231		X		X	X	X	X	
<i>Szepligetella</i> 233	233		X	X	X	X	X	X	
<i>Szepligetella</i> 236	236		X	X	X	X		X	
<i>Szepligetella</i> 238	238		X	X	X	X	X	X	
<i>Szepligetella</i> 241	241				X	X	X	X	
<i>Szepligetella</i> 243	243		X	X	X		X	X	
<i>Szepligetella</i> 247	247				X		X	X	
<i>Szepligetella</i> 248	248		X		X		X	X	
<i>Szepligetella sericea</i>	297					X	X	X	
<i>Szepligetella</i> 047	208	047	D	X	X		X	D	D
<i>Szepligetella</i> 055	280	055		X	X		X	D	D
<i>Szepligetella</i> 056	294	056	D	X	X	X	X	X	D
<i>Szepligetella</i> 285	285			X	X	X	X	X	
<i>Trissevania anemotis</i>	282	038	D	X		X	X	D	D
<i>Trissevania</i> 507	507					X			
<i>Zeuxevania</i> 499	499				X	X			
<i>Zeuxevania</i> 500	500				X	X		X	
<i>Zeuxevania</i> 503	503					X			
<i>Zeuxevania</i> 505	505		X		X	X	X	X	
<i>Zeuxevania</i> 015	191	015	D		X			D	D
<i>Zeuxevania splendidula</i>	312	031	D		X	X	X	X	D
% amplified			71	44	66	64	67	86	50
% parsimony-informative			40	44	49	53	35	60	40

Table 1. Taxonomic and genetic sampling. Exemplars used by Deans et al. (2006) are listed with the reference from that paper (DV#) beside the internal voucher number (Ext.) Genes for each taxon are marked with an **X** if amplified in this study and **D** if amplified by Deans et al. (2006). Gene codes: 28S = 28S rDNA; AM2 = alpha-mannosidase II; CAD1 and CAD2 = carbamoyl-phosphate synthetase-aspartate transcarbamoylase-dihydroorotase (CAD) (for amplicon regions for each segment, see Figure 1); RPS23 = Ribosomal Protein S23; COI = cytochrome oxidase I; 16S = 16S rDNA.

99

100 Each exemplar not identified to species represents a putative morphospecies, as many species remain

101 undescribed. Several DNA extracts and some sequences were used from Deans et al. (2006), as indicated
102 in Table 1. Vouchers were deposited at the Frost Entomological Museum, at The Pennsylvania State
103 University, or in repositories stipulated by collecting permits and/or loan agreements. See supplementary
104 CSV file (EvaniidPhylogenyVouchers.csv).

105 **Gene selection**

106 We utilized DNA from six different genes, including two mitochondrial (mt) genes (16S ribosomal DNA
107 (*16S*) and cytochrome c oxidase I (*COI*)) and four nuclear genes (28S ribosomal DNA (*28S*), ribosomal
108 protein S23 (*RPS23*), carbamoyl-phosphate synthetase-aspartate transcarbamoylase-dihydroorotase (*CAD*)
109 and alpha-mannosidase II (*AM2*)). Diagrams of the gene structures of *CAD*, *RPS23*, and *AM2* are
110 presented in Figure 1. The diagrams were produced based on annotations of the genomic reference
111 sequences from *Apis mellifera* Linnaeus, 1758 (NCBI RefSeq ID: GCF_000002195.4) and *Nasonia*
112 *vitripennis* (Ashmead, 1904) (NCBI RefSeq ID: GCF_000002325.3), visualized in NCBI's Sequence
113 Viewer (<http://www.ncbi.nlm.nih.gov/tools/sviewer>) and Geneious v.6.0.6 (Biomatters
114 Ltd.) The annotations include information on the introns, exons, organization of coding regions and
115 protein product features. Conserved domains in the protein products were also identified via a BLASTx
116 search (Altschul et al., 1990) against NCBI's Conserved Domains Database (CDD) (Marchler-Bauer
117 et al., 2015). The genetic regions corresponding to the identified domains are included for reference in
118 the diagrams as well as the primers used in this study (primer sequences are listed in Table S2). Further
119 background about the three protein coding genes is provided below since the amplified regions or genes
120 utilized are novel for phylogenetic studies. All sequences are available in NCBI's Genbank (<https://www.ncbi.nlm.nih.gov/genbank/>)
121 under accession numbers KY082187–KY082565.

122 **CAD**

123 *CAD* is a long and complex gene which codes a “fusion” protein, that is, a protein with multiple
124 enzymatic activities: glutamine-amidotransferase (GATase), carbamoylphosphate synthetase (CPSase),
125 dihydroorotase (DHOase) and aspartate/ornithine transcarbamoylase (ATCase/OTC). There are 26 exons
126 and 25 introns in both *Apis* and *Nasonia*, although intron loss has been reported in the CPSase small chain
127 region in some Braconidae (Sharanowski et al., 2011). CPSase is divided in two domains: one for a short
128 chain, which includes GATase, and one for a long chain. The long chain is also subdivided, consisting
129 of two subunits (N-terminal + ATP-binding region), one oligomerization domain, and one MGS-like
130 (methylglyoxal synthetase-like) domain. These two CPSase chains are coded by 14 exons. Various
131 segments of this gene have been used in other phylogenetic studies of insects, particularly for lineages
132 diversifying within the last 150 million years (Danforth et al., 2006; Moulton and Wiegmann, 2004;
133 Winterton and De Freitas, 2006). The regions we analyzed are within the CPSase domains, extending
134 between exons 3 to 5 (Figure 1A).

135 **RPS23**

136 Ribosomal protein S23 (Figure 1B) is part of the small ribosomal subunit (Wool, 1979). It has a binding
137 site for mRNA and is associated with the eukaryotic initiation factor of the translation process (NCBI-
138 CDD:cd03367). This gene has been previously used in macro-evolutionary phylogenetic studies on
139 Hymenoptera (Sharanowski et al., 2010) and Arthropoda (Aleshin et al., 2009; Timmermans et al., 2008)
140 and as an EPIC (exon-primed, intron-crossing) marker for population-level studies (Lohse et al., 2011,
141 2010). RPS23 is well conserved in sequence and structure across Hymenoptera, with the variation
142 concentrated in the introns. In both *Apis* and *Nasonia*, there are three exons (3bp, 159bp, and 270bp
143 in length) and 2 introns (339bp and 84bp in *Apis*; 353bp and 79bp in *Nasonia*). The amplified region
144 covers the downstream region of exon 2, full intron 2, and about half of exon 3, which contains the
145 aminoacyl-tRNA interaction site and therefore is expected to be conserved.

146 **AM2**

147 We performed sequence similarity searches with tBLASTx (Altschul et al., 1990), using Hymenopteran
148 expressed sequence tags (ESTs) from Sharanowski et al. (2010) against proteins of *Apis mellifera* and
149 *Nasonia vitripennis*. Our search focused on genes with regions of variability (for putative phylogenetic
150 signal), limited introns and relatively long exons, and regions of sequence conservation (for priming sites).
151 Alpha-mannosidase II is a glycoside hydrolase involved in the catabolism of carbohydrates (Gonzalez and
152 Jordan, 2000) and has not been explored for phylogenetic studies. There has been a shift in the placement
153 of the second intron between *Nasonia* and *Apis* (Figure 1C), and thus we labeled the exons 2a and 2b

154 to demonstrate the homology with labeled exon 3 in both taxa. Three main protein domain regions are
155 identifiable in the reference sequences: (1) an N-terminal catalytic domain of Golgi alpha-mannosidase II,
156 which is entirely in exon 2a in *Apis*, but overlaps the second intron in *Nasonia*, and therefore also lies in
157 exon 2b; (2) a middle domain, which is located in exon 3; and (3) and a C-terminal, which is located in
158 exon 4 (Figure 1C). The amplified area is contained in the region that corresponds to the N-terminal in
159 *Apis*, ending before the second intron (Figure 1C). No intron was amplified in the evanioid taxa used in
160 this study, and thus the gene structure is more similar to *Apis* in the amplified region.

161 Extraction and Sequencing

162 Extraction of genomic DNA was performed following the manufacturer's protocols using the DNeasy™
163 Tissue Kit (Qiagen, USA). Exemplars were either whole body extracted or only the separated thorax
164 and metasoma were used as the use of the head often resulted in low DNA concentrations in Evaniids.
165 *COI* was amplified using the protocols outlined in Schulmeister et al. (2002), with the primers developed
166 for that study or using the universal primers developed by Folmer et al. (1994) and following protocols
167 outlined in Namin et al. (2014) (Table S2). Sequences for 16S mitochondrial rDNA were used from Deans
168 et al. (2006), which were based on primers and protocols developed in previous studies (Dowton and
169 Austin, 1994; Whitfield, 1997). Amplification of the D2-D3 region of 28S was performed using either
170 primers developed by Dowton and Austin (2001) or primers newly developed for this study (Table S2),
171 due to difficulty with amplification of some taxa. *CAD* sequences were amplified in two discontinuous
172 fragments using newly developed primers (Figure 1; Table S2: *CAD1*, *CAD2*). For *CAD1*, three reverse
173 primers were developed to either reduce degeneracy or due to amplification difficulties in some taxa, and
174 a touchdown protocol was also used to increase specificity of the reaction (Table S2). For *CAD2*, two sets
175 of primers were developed, the second set (CAD-Amel379F/CAD-Amel479R) slightly internal to the
176 first (CAD-Amel368F/CAD-Amel482R). If no amplification product was achieved with the first set of
177 primers, the second set was used alone or as a nested re-amplification of the product obtained with the
178 first set. *RPS23* was amplified using primers developed by Lohse et al. (2011) and in conjunction with
179 a second newly developed reverse primer and amplified with a touchdown protocol (Figure 1B; Table
180 S2). Primers were also designed to amplify AM2, with an internal forward primer (AM2-Amel1356F)
181 amplifying a much shorter fragment (Figure 1C, Table S2), which increased the number of taxa for which
182 we achieved amplification success.

183 All PCR amplifications were carried out using 0.2–1 μg DNA extract, 1× Standard Taq Buffer (New
184 England Biolabs, USA) (10 mM Tris-HCl, 50 mM KCl, 1.5 mM MgCl₂), 200 μM dNTP, 4 mM MgSO₄,
185 400 nM of each primer, 1 unit of Taq DNA polymerase (New England Biolabs, USA) and purified water to
186 a final volume of 25 μL. PCR products were visualized on a 1% agarose gel. Occasionally 5% Dimethyl
187 sulfoxide (DMSO, Sigma-Aldrich, USA) was added as a PCR additive when non-specific bands occurred.
188 This additive has been shown to increase PCR yield with GC-rich templates (Farell and Alexandre, 2012).
189 Nested re-amplifications were performed using 0.5 μL of PCR product as DNA template (concentrations
190 varied depending on first PCR reaction success). PCR purification was performed using ExoSAP-IT
191 (Affymetrix, USA) following the manufacturer's instructions, except using 25% of the suggested reagent
192 amount. If double bands were visualized on the gel following PCR, a subsequent 50 μL reaction was run
193 on gel cut bands, the product ran on a 2.5% agarose gel, and purified using the QIAquick Gel Extraction
194 Kit (Qiagen, USA) following the manufacturer's protocols. Sequencing was carried out using the BigDye
195 Terminator v 3.1 Cycle Sequencing Kit (Applied Biosystems, U.S.A.), with reaction products sequenced
196 on an Applied Biosystems 3730xl DNA Analyzer at the Genomic Sciences Laboratory, North Carolina
197 State University. Contigs were assembled and trimmed for quality using Geneious.

198 Sequence alignment

199 The protein-coding genes were aligned by translating the sequences and setting the correct reading frame
200 in BioEdit (Hall, 1999). Sequences were then aligned as proteins using MAFFT (Katoh and Standley,
201 2013) on the EMBL-EBI webserver (Li et al., 2015) under default settings and then back translated
202 to nucleotides. Introns present in *CAD1* and *RPS23* were excluded from the dataset prior to multiple
203 sequence alignment. Ribosomal DNA sequences were aligned following secondary structure models
204 developed by Gillespie et al. (2005a,b) and modified by Deans et al. (2006) for Evaniidae. Regions of
205 ambiguous alignment (RAA), expansion and contraction (REC), and slipped-strand compensation (RSC)
206 were excluded from the analysis, following Deans et al. (2006). For analysis of sequence motifs, intron

207 were aligned using MAFFT with a gap opening penalty of 2 and gap extension penalty of 0.5 to limit
208 excessive gaps in the alignment.

209 **Phylogenetic analyses**

210 The optimal partitioning scheme and models of evolution for the concatenated analysis were determined
211 using PartitionFinder v.1.1.1 (Lanfear et al., 2012). Character sets were predefined by gene, and by codon
212 position for the 5 protein-coding genes for a total of 17 partitions (*CAD1* and *CAD2* were partitioned
213 separately). The Bayesian information criterion was used to select among models implemented in
214 MrBayes version 3.2 Ronquist et al. (2012b), with the greedy search algorithm and branch lengths
215 unlinked. The optimal scheme included two partitions. The first partition included the 3rd codon positions
216 for *CAD1*, *CAD2*, *AM2*, and *RPS23* under the Hasegawa-Kishino-Yano model (Hasegawa et al., 1985).
217 The remaining 13 predefined partitions were included together under the general time reversible model
218 (GTR). Both partitions included a parameter for invariant sites and rate heterogeneity modeled under a
219 gamma distribution. We observed notable differences in nucleotide composition across taxa for some
220 genes (calculated in MEGA v.6 Tamura et al., 2013), and thus, tested for base composition homogeneity
221 using chi-square tests in PAUP* (Swofford, 2002) (Supplementary Material Table S3). For *CAD1* and
222 *RPS23* the intron was removed.

223 Phylogenies were estimated using MrBayes 3.2, either on the CIPRES Science Gateway (Miller et al.,
224 2010) or the ComputeCanada WestGrid computational facility. Parameters were unlinked and site specific
225 rates were allowed to vary across partitions. Analyses were performed with two independent searches
226 and four chains. All concatenated analyses were run for 10 million generations, sampling every 2000th
227 generation. Individual gene trees were analyzed with 5 million generations, sampling every 1000th.
228 Convergence diagnostics, stationarity, and appropriate mixing were assessed with Tracer v1.6 (Rambaut
229 and Drummond, 2009), and a suitable burn-in was chosen based on the parameter values. Trees from
230 the posterior distribution were summarized post burn-in with a majority rule consensus and manipulated
231 for better visualization using FigTree v.1.3.1 (Rambaut, 2012) and modified for publication using Adobe
232 Illustrator (Adobe Systems, Inc. San Jose, CA). The final nexus file is available through Penn State's
233 ScholarSphere repository (DOI: 10.18113/S1D06H).

234 **Divergence time estimations**

235 An uncorrelated log-normal relaxed clock as implemented in the program BEAUTi and BEAST v.1.8.2
236 (Drummond et al., 2002, 2012) was used to estimate divergence times. The same partitions and models
237 of molecular evolution were applied to each partition as in the phylogenetic analysis. We utilized the
238 Birth-Death process for incomplete sampling (Stadler, 2009) and started with a random tree. Only
239 the calibration for the entire ingroup (Evaniiidae) was constrained to be monophyletic which was well
240 supported from the Bayesian analysis.

241 We utilized six fossil calibration points with each fossil assigned to the crown group for which they
242 belonged (see Fossil Calibrations in Supplementary Material) (Brues, 1933; Nel et al., 2002; Peñalver et al.,
243 2010; Jennings et al., 2004, 2013; Jennings and Krogmann, 2009; Rasnitsyn et al., 1998; Sawoniewicz
244 and Kupryjanowicz, 2003). We performed two separate analyses to examine uncertainty with respect to
245 maximum bounds for clade ages. For the first analysis we used log-normal distributions. The age of the
246 fossil determined the hard minimum bound, as the clade to which it belongs must be at least that old. We
247 then chose a mean and standard deviation so that the 95% highest priority density interval (95% HDP)
248 for the divergence estimation of the clade was from 2 to 25 million years prior to the age of the fossil. The 25
249 million year demarcation is arbitrary, but it seems reasonable and follows Cardinal and Danforth (2013).
250 For the second analysis we chose hard maximum bounds based on previous knowledge of the fossil record
251 and the evolutionary relationships among the included taxa, which are justified (Supplementary Material
252 – Fossil Calibrations) for each calibration. Generally, we chose the mean as the average between the
253 hard minimum and maximum bounds and then set the standard deviation so that the 95% HDP spanned
254 the range from the minimum to the maximum bound. For both analyses, initial values were set to the
255 mean and the ucl.d.mean prior was set to exponential with a mean of 0.05. Although these values are
256 somewhat arbitrary, according to the authors of the program, they are unlikely to have an effect on
257 the analysis (Drummond and Rambaut, 2007; Drummond et al., 2012). All other parameters and the
258 Markov-chain Monte Carlo settings were left at the default settings. The xml input files for both the
259 lognormal and normal distribution analyses are available through Penn State's ScholarSphere repository
260 (DOI: 10.18113/S1D06H).

261 RESULTS AND DISCUSSION

262 Phylogenetic analyses

263 The final concatenated data set consisted of 3097 characters total: *COI* (681bp), *16S* (371bp, excluding
264 RAAs), *28S* (428bp, excluding RAAs), *AM2* (672bp), *CAD1* (417bp, excluding the intron), *CAD2* (321bp),
265 and *RPS23* (207bp, excluding the intron). Individual gene trees are depicted in Supplementary Figures
266 S1-S7. The null hypothesis for base composition homogeneity was rejected for *AM2* ($\chi^2 = 368.819$,
267 $df = 120$; $P = 0.000000000$) and *COI* ($\chi^2 = 562.535$, $P = 0.0000000$) (Table S3). Average nucleotide
268 composition across all genes and gene regions analyzed are depicted in Table S3.

269 The Bayesian analysis of the concatenated dataset recovered a well resolved tree with most clades
270 well supported ($pp > 0.95$) (Figure 2). Clades recovered across the individual gene trees and for the
271 concatenated analysis are summarized in Table S4 and gene trees are depicted in Figures S1-S7. We
272 also performed a Maximum Likelihood analysis with RaxML v8.2.4 (Stamatakis, 2014, 2006) (Figure
273 S15) under the GTR+CAT model and auto-determination of bootstrap replicates. The phylogenies
274 obtained from BEAST (Figure 3), Mr.Bayes (Figure 2), and RaxML (Figure S15) were very similar except
275 relationships among species varied within genera and *Micreвания* was not monophyletic in the Bayesian
276 analysis (Figure 2). The placement of *Rothevania* also varied across analyses.

277 In the concatenated analysis (Figure 2), Evaniidae was recovered as monophyletic with high support
278 ($pp = 1.0$). Of the 15 genera included in the analysis with more than one representative, nine were
279 recovered as monophyletic, including *Evaniscus*, *Decevania*, *Semaemyia*, *Evania*, *Hyptia*, *Brachygaster*,
280 *Prosevania*, *Trissevania*, and *Evaniella*. All clades representing monophyletic genera had posterior
281 probabilities of 1.0. Although *Micreвания* was recovered as paraphyletic, it was recovered as monophyletic
282 in other analyses, as mentioned above, the divergence analysis (Figure 3), ML analysis (Fig S.15) and
283 the *16S* and *COI* individual gene analyses (Table S3) and previously by Deans et al. (2006).

284 Similar to the previous study (Deans et al., 2006), *Parevania* and *Zeuxevania* were recovered as
285 paraphyletic with respect to each other, but in a well-supported clade ($pp = 1.0$) with *Papatuka*, in the
286 concatenated analysis as well as five of the seven gene trees (Table S4). Interestingly, all of these taxa
287 have a distinct sequence motif at the 3' end of the *RPS23* intron: GTTTGTTTTG YAG (Fig. S9). No other
288 evaniid taxa have a similar motif at the 3' end (Fig. S8), and thus the motif is diagnostic for this clade.
289 *Trissevania* and *Evania* were recovered as sister taxa with high support ($pp = 1.0$) in the concatenated
290 analysis and these two taxa were recovered as sister to *Zeuxevania* + *Parevania* + *Papatuka* ($pp = 0.98$)
291 (Figure 2). But there was little support for these higher level relationships among in the individual gene
292 trees (Table S4). *Brachygaster* was recovered as sister to *Prosevania* with strong support ($pp = 1.0$) but
293 was only recovered in the *CAD2* gene tree (Fig. S4). *Micreвания* was also recovered as the sister to
294 all remaining evaniids, followed by *Brachygaster* + *Prosevania* in the concatenated analysis. Yet, the
295 position of these taxa fluctuated widely among the individual gene trees, likely due to inconsistent taxon
296 sampling across the gene trees.

297 *Acanthinevania* and *Szepligetella* were consistently recovered together ($pp = 1.0$ in the concatenated
298 analysis (Figure 2) and all gene trees except *16S* (Table S4), but were paraphyletic with respect to
299 each other. Interestingly, all members of *Acanthinevania* and *Szepligetella* have a GATCTAAC motif
300 (Fig. S10) in the *RPS23* intron that is not shared with any other evaniid taxa (Fig. S8), highlighting
301 their close evolutionary relationship. There are also two diagnostic motifs within regions of ambiguous
302 alignment (RAAs) that were excluded from the phylogenetic analyses. All members of *Acanthinevania* and
303 *Szepligetella* have the motif TAAAAT in RAA8 (Fig. S11) and the motif TGCA YT within RAA12 (Fig.
304 S12). *Evaniella* was recovered as the sister group to *Acanthinevania* + *Szepligetella* in the concatenated
305 analysis and in three genes trees (Table S4). Members of all three genera share a 9bp diagnostic motif in
306 RAA10 in *28S*: YTCGAWAAA (Fig. S12). Most other evaniid taxa do not have this many base pairs in
307 this position (usually 2–4bp); the ones that do have longer motifs are radically different in sequence (the
308 full alignment is available in Scholarsphere, DOI:10.18113/S1D06H). *Alobevania* was recovered as sister
309 to *Evaniella* + (*Acanthinevania* + *Szepligetella*), with strong support in the concatenated analysis, and
310 with moderate support ($pp = 0.88$) in the *28S* gene tree. This result is unsurprising given that these taxa
311 were once treated as *Evaniella* (Deans and Huben, 2003).

312 New world taxa with reduced wing venation (*Evaniscus*, *Decevania*, *Hyptia*, *Rothevania*, and *Se-*
313 *maemyia*) are recovered together in a well-supported clade ($pp = 1.0$), in the concatenated analysis
314 (Figure 2). This clade is only recovered in the *CAD1* gene tree (Figure S4), possibly due to lower taxo-
315 nomic sampling in some individual gene trees due to failed amplification. However, these taxa are present

316 in various combinations throughout the individual gene trees, but the relationships among taxa fluctuate
 317 widely, which is also reflected in the lower support values in the concatenated tree for relationships among
 318 these genera (Figure 2).

319 Divergence time analyses

320 The phylogenies obtained from the two Bayesian uncorrelated relaxed clock analyses using BEAST were
 321 both identical (Figure 3 (simplified chronogram from the log-normal distribution) and Fig S14 (normal
 322 distribution)). Other than slight differences among species within genera, and the recovery of *Micrevania*
 323 as monophyletic, the trees were very similar to the tree obtained from the analysis with MrBayes (Figure
 324 2). Estimates of divergence time from both analyses, using either a log-normal and normal distribution
 325 are listed in Table 2. The log-normal analysis estimated younger divergence times for all clades (Table
 326 2). This was expected as the calibration bounds were constrained within 25 million years of the fossil's
 327 age in the log-normal analysis, but were allowed to vary across a larger span of time in the normal
 328 distribution analysis based on interpretations of the fossil record. It is likely that the normal analysis
 329 uses too broad a range, with the maximum bound being set too far away from the oldest known fossil
 330 for the crown lineage, and thus we depict the log-normal analysis (Figure 3) and use these dates to draw
 331 inferences about evaniid clade divergence. Evaniidae was estimated to diverge around 137 million years
 332 ago (Mya) (134.1–141.1). Although the superfamily was not the focus of this study, Evanioidea had
 333 an estimated mean age of 168 Mya (135.9–199.0), consistent with other previous estimates suggesting
 334 Evanioidea diverged in the mid-late Jurassic (Peters et al., 2017; Branstetter et al., 2017). Branches
 335 leading to *Micrevania*, *Prosevania*, and *Brachygaster* split sometime around the end of the Cretaceous,
 336 with means ranging between 60–73 Mya (Table 2). Other extant genera likely diverged sometime in the
 337 early Cenozoic and these lineages were likely all present before the start of the Neogene (Figure 3, Table
 338 2).

	Log-normal - Age (My) mean (95% HDP)	Normal - Age (My) mean (95% HDP)
<i>Gasteruption</i> (Gasteruptionidae)	38.6 (18.5–59.3)	46.3 (27.2–69.4)
<i>Pristaulacus</i> (Aulacidae)	49.1 (45.4–54.7)	48.9 (23.3–73.6)
Evaniidae	136.8 (134.1–141.4)	151.5 (135.9–166.7)
<i>Brachygaster</i>	60.7 (40.5–86.4)	72.1 (49.5–96.3)
<i>Decevania</i>	37.6 (25.2–51.1)	47.8 (31.6–64.0)
<i>Evania</i>	45.3 (33.3–58.6)	55.4 (40.5–70.7)
<i>Evaniella</i>	69.3 (55.5–84.0)	88.6 (73.5–104.3)
<i>Evaniscus</i>	66.0 (40.8–89.5)	80.4 (50.1–110.3)
<i>Hyptia</i>	50.7 (45.7–57.8)	65.4 (50.7–81.2)
<i>Micrevania</i>	67.8 (38.4–94.8)	80.1 (52.5–111.8)
<i>Prosevania</i>	72.1 (58.6–86.4)	85.7 (67.6–103.8)
<i>Semaeomyia</i>	59.0 (46.6–72.5)	76.9 (61.1–94.0)
<i>Szepligetella s.l.</i>	49.0 (38.3–60.1)	60.6 (48.6–72.1)
<i>Trissevania</i>	32.0 (17.5–50.4)	38.5 (20.5–57.3)
<i>Zeuxevania s.l.</i>	55.6 (45.8–66.3)	76.0 (59.6–92.2)

Table 2. Estimates of divergence times for Evaniidae (bolded) and outgroups based on an uncorrelated log-normal relaxed clock analyses. Six fossil calibrations were used (see Supplementary Material) with maximum bounds for clade ages set using a log-normal (Analysis 1) and normal distribution (Analysis 2). For each analysis the mean age in millions of years (My) and the 95% highest posterior density interval (HDP, equivalent to a confidence interval) is provided.

339 Novel genes and molecular signatures

340 *Alpha-mannosidase 2* (*AM2*) has never been used before in phylogenetic studies. This gene has a mix of
 341 conserved and variable sites (44% parsimony-informative sites), but it failed the test for base composition
 342 homogeneity, which can cause systematic biases in phylogenetic analyses (Phillips et al., 2004; Rodríguez-
 343 Ezpeleta et al., 2007; Sharanowski et al., 2011). RY-coding this gene did not change the results obtained

344 from the concatenated analysis. Unfortunately amplification of *AM2* was difficult, even with the addition
 345 of PCR additives such as DMSO, causing a high amount of missing data. Gel cuts were often necessary
 346 to achieve clean sequences for several genes, but particularly *AM2*. *RPS23* was highly conserved in the
 347 exonic regions, and thus may be better suited for deeper level studies across families. There were distinct
 348 molecular signatures within the intronic region that would be very useful for lower level studies, such as
 349 across species, or population-level studies (see Lohse et al., 2010). The molecular motifs in the *RPS23*
 350 intron were useful for delimiting genera and diagnosing congenics (see taxonomic implications, below).
 351 The individual gene trees for both regions of *CAD* were relatively well resolved (Figures S4-5) and similar
 352 to other studies (Desjardins et al., 2007; Sharanowski et al., 2011), which demonstrates good utility for
 353 resolving phylogenetic relationships in Hymenoptera.

354 Alignments based on secondary structure for rDNA have been very useful for delimiting highly
 355 variable regions to exclude from analyses to achieve better phylogenetic results (Gillespie et al., 2005b;
 356 Pitz et al., 2007). However, variable regions have useful information with phylogenetic and taxonomic
 357 utility, as demonstrated by Sharanowski et al. (2011), who included variable regions (RECs, RAAs, and
 358 RSCs) if the variation in sequence length had a standard deviation less than one. Here we demonstrate the
 359 utility of some of these regions for diagnosing genera (Figures S11-12) and use these data to improve
 360 taxonomic classifications (see Taxonomic implications below).

361 Taxonomic implications

362 Relative to the Deans et al. (2006) study, the addition of several more genes and taxa clearly led to
 363 increased resolution. For example, an additional four genera were recovered as monophyletic, and higher
 364 level relationships were more resolved and better supported. Our understanding of evaniid relationships
 365 remains incomplete, but, based on mounting evidence here and through our observations of morphology,
 366 we feel comfortable proposing the following classificatory changes.

367 **New synonyms of *Zeuxevania* and new combinations** *Parevania*, **syn. nov.**, and *Papatuka*, **syn.**
 368 **nov.**, are congeneric with and junior synonyms of *Zeuxevania*. Bradley (1908) also suspected that these
 369 two taxa were congeneric and treated *Parevania* as a subgenus of *Zeuxevania*. These taxa are consistently
 370 recovered together in well-supported clades across individual gene trees and within the concatenated
 371 analyses, but are polyphyletic with respect to each other (Table S4). Additionally, there are molecular
 372 signatures within the *RPS23* intron that support their shared evolutionary history (Fig. S9). ARD has
 373 observed thousands of specimens of these taxa and can find no consistency in the presence or absence of
 374 the fore wing vein 1RS, which was the only character purported to separate *Parevania* and *Zeuxevania*
 375 (Deans and Huben, 2003).

376 Following the taxonomy of Hedicke (1939), we hereby transfer the following species back to *Zeuxe-*
 377 *vania*: *albitarsus* (Cameron, 1899); *annulicornis* (Turner, 1927); *atra* (Kieffer, 1916); *bisulcata* (Kieffer,
 378 1911); *curvicarinata* (Cameron, 1899); *kriegeriana* (Enderlein, 1905); *leucostoma* (Kieffer, 1910); *longi-*
 379 *calcar* (Kieffer, 1911); *punctatissima* (Kieffer, 1911); *rubra* (Cameron, 1905); *sanguineiceps* (Turner,
 380 1927); *schlettereri* Bradley 1908; *schoenlandi* (Cameron, 1905); *semirufa* (Kieffer, 1907).

381 We also transfer the following species to *Zeuxevania* for the first time: *aurata* (Benoit, 1950), **comb.**
 382 **nov.**; *brevis* (Brues, 1933), **comb. nov.**; *broomi* (Cameron, 1906), **comb. nov.**; *emarginata* (Kieffer,
 383 1911), **comb. nov.**; *kasauliensis* (Muzaffer, 1943), **comb. nov.**; *laeviceps* (Enderlein, 1913), **comb. nov.**;
 384 *madegassa* (Benoit, 1952), **comb. nov.**; *meridionalis* (Cameron, 1906), **comb. nov.**; *micholitzi* (Enderlein,
 385 1905), **comb. nov.**; *ortegae* (Ceballos, 1966), **comb. nov.**; *plana* (Benoit, 1952), **comb. nov.**; *producta*
 386 (Brues, 1933), **comb. nov.**; *remanea* (Brues, 1933), **comb. nov.**.

387 *Papatuka* was originally described from a single, apterous specimen (Deans, 2002) and was since
 388 expanded to include other, winged species (Deans, 2005). The morphology of these species, which is
 389 also reflected in the molecular data, is not substantially different from *Zeuxevania*, and we transfer those
 390 species to *Zeuxevania*: *alamunyiga* (Deans, 2002), **comb. nov.**; *capensis* (Schletterer, 1886), **comb. nov.**;
 391 *longitarsis* (Kieffer, 1904), **comb. nov.**

392 **New synonym of *Szepligetella* and new combinations** There is also abundant evidence to support
 393 *Acanthinevania* as congeneric with *Szepligetella*. They are consistently recovered together in a clade but
 394 neither appears to be monophyletic by itself (Table S4). The primary diagnostic characters that separated
 395 these two primarily Australian genera include: *Szepligetella* with the third labial palpomere swollen;
 396 *Acanthinevania* with an elongated head relative to *Szepligetella*; and *Acanthinevania* with labium folded

397 strongly anteriorly and thus appearing long and narrow, not broad and flat as in most *Szepligetella* (Deans
398 and Huben, 2003). Our observations of more than 1,000 specimens reveal that these character states (e.g.,
399 face long vs. face short) fall along phenotypic gradients, with no discrete sets of states. Several molecular
400 characters link (but do not separate) these genera, including motifs present in the *RPS23* intron and at
401 least two regions of 28S (Figs S10-12).

402 We treat *Acanthinevania*, **syn. nov.**, as *Szepligetella* and transfer the following species to *Szepligetella*:
403 *australis* (Schletterer, 1886), **comb. nov.**; *braunsi* (Kieffer, 1911), **comb. nov.**; *braunsiana* (Kieffer,
404 1911), **comb. nov.**; *clavaticornis* (Kieffer, 1911), **comb. nov.**; *erythrogaster* (Kieffer, 1904), **comb. nov.**;
405 *eximia* (Schletterer, 1886), **comb. nov.**; *genalis* (Schletterer, 1886), **comb. nov.**; *humerala* (Schletterer,
406 1889), **comb. nov.**; *leucocras* (Kieffer, 1911), **comb. nov.**; *longigena* (Schletterer, 1889), **comb. nov.**;
407 *lucida* (Schletterer, 1889), **comb. nov.**; *mediana* (Schletterer, 1889), **comb. nov.**; *princeps* (Westwood,
408 1841), **comb. nov.**; *quinclineata* (Kieffer, 1904), **comb. nov.**; *rufiventris* (Kieffer, 1911), **comb. nov.**;
409 *scabra* (Schletterer, 1889), **comb. nov.**; *sericans* (Westwood, 1851), **comb. nov.**; *striatifrons* (Kieffer,
410 1904), **comb. nov.**; *szepligeti* (Bradley, 1908), **comb. nov.**; *versicolor* (Kieffer, 1904), **comb. nov.**;
411 *villosicrus* (Kieffer, 1904), **comb. nov.**

412 **Emerging tribal classification** A new tribal classification for Evaniidae is warranted, given the lack of
413 support for Bradley's (1908) original (>100 year-old) tribal concepts (Deans, 2005; Deans et al., 2006;
414 Deans and Huben, 2003). Mikó et al. (2014) recently described *Trissevaniini*, to include *Trissevania* and
415 *Afrevania*, and, based on our results here, molecular work by (Deans et al., 2006), and prior morphological
416 work by us and our colleagues (Deans and Huben, 2003; Deans and Kawada, 2008; Kawada and Azevedo,
417 2007; Kawada, 2011) we have an opportunity to revise Hyptiini to include those New World genera
418 with reduced wing venation: *Evaniscus*, *Hyptia*, *Rothevania*, *Semaeomyia*, and *Decevania*. We remove
419 *Brachygaster*, *Evaniella*, and *Zeuxevania* from Hyptiini (see Bradley, 1908). This updated concept of
420 Hyptiini can be separated from other evaniid taxa by the absence of at least the fore wing RS+M, and
421 usually many other apical veins (see Figs. 1, 9, 11, 16, 17 in Deans and Huben, 2003), and its origin in
422 the New World.

423 **Evaniid divergence and evolution**

424 Evaniids diverged in the Early Cretaceous (ca. 134.1–141.1 Mya), when numerous modern cockroach
425 fossils have been found (Grimaldi and Engel, 2005), although cockroaches with oothecae are thought
426 to have much earlier origins in the Late Carboniferous (Legendre et al., 2015). Most of the extant
427 evaniid genera diverged sometime near the K-T boundary, which may indicate that the mass extinction
428 played a role in the divergence of multiple new lineages of ensign wasps. Whether or not there has been
429 co-cladogenesis with modern cockroach lineages remains to be tested but would be hampered by the lack
430 of known host relationships for most evaniids (Deans, 2005). For evaniids, as for most Hymenoptera,
431 basic natural history research is needed to understand the trophic relationships among wasps and their
432 hosts.

433 **CONCLUSION**

434 We provide here a more robust and well-resolved phylogeny for Evaniidae than previous studies, which
435 will facilitate ongoing evolutionary and taxonomic work. Indeed, the new synonyms and combinations
436 proposed above help us progress towards a stable classification that reflects evolutionary relationships.
437 Building on prior results (Deans et al., 2006), our data also reveal new, useful markers for Hymenoptera
438 (*AM2* and *RPS23*) and continue to support the utility of shared molecular motifs in defining major clades
439 in Evaniidae. Our results indicate that Evaniidae diverged in the early Cretaceous with most genera
440 diversifying in the late Cretaceous or early Tertiary. The results also highlight important targets for future
441 data collection, especially near the base of the tree (*Micrevania*) and the relationships within each genus.
442 More intensive sampling, especially with the addition of morphological data and fossils (e.g., Ronquist
443 et al., 2012a), is the logical next step in providing a tribal classification and more refined estimates for
444 divergence times.

445 **ACKNOWLEDGMENTS**

446 We are grateful to Mike Irwin, Martin Hauser, Kevin Holston, Jack Longino, Mike Sharkey, the late Evert
447 Schlinger, the late Don Webb, and countless other collectors who shared material with us. We also thank

448 the numerous loan facilitators, without whom this work would be impossible and the three reviewers who
449 helped improved the manuscript.

450 REFERENCES

- 451 Aleshin, V., Mikhailov, K., Konstantinova, A., Nikitin, M., Rusin, L. Y., Buinova, D., Kedrova, O., and
452 Petrov, N. (2009). On the phylogenetic position of insects in the Pancrustacea clade. *Molecular Biology*,
453 43(5):804–818.
- 454 Altschul, S. F., Gish, W., Miller, W., Myers, E. W., and Lipman, D. J. (1990). Basic local alignment
455 search tool. *Journal of molecular biology*, 215(3):403–410.
- 456 Balhoff, J. P., Mikó, I., Yoder, M. J., Mullins, P. L., and Deans, A. R. (2013). A semantic model for species
457 description applied to the ensign wasps (Hymenoptera: Evaniidae) of New Caledonia. *Systematic
458 Biology*, 62(5):639–659.
- 459 Bradley, J. C. (1908). The Evaniidæ, ensign-flies, an archiac family of Hymenoptera. *Transactions of the
460 American Entomological Society*, 34(2):101–194.
- 461 Branstetter, M. G., Danforth, B. N., Pitts, J. P., Faircloth, B. C., Ward, P. S., Buffington, M. L., Gates,
462 M. W., Kula, R. R., and Brady, S. G. (2017). Phylogenomic insights into the evolution of stinging
463 wasps and the origins of ants and bees. *Current Biology*, 27(7):1019–1025.
- 464 Brues, C. T. (1933). The parasitic Hymenoptera of the Baltic amber. part 1. *Bernstein-Forschungen*,
465 3:4–172.
- 466 Cardinal, S. and Danforth, B. N. (2013). Bees diversified in the age of eudicots. *Proceedings of the Royal
467 Society of London B: Biological Sciences*, 280(1755).
- 468 Danforth, B. N., Fang, J., and Sipes, S. (2006). Analysis of family-level relationships in bees (Hy-
469 menoptera: Apiformes) using 28S and two previously unexplored nuclear genes: CAD and RNA
470 polymerase II. *Molecular Phylogenetics and Evolution*, 39(2):358–372.
- 471 Deans, A. and Huben, M. (2003). Annotated key to the ensign wasp (Hymenoptera: Evaniidae) genera
472 of the world, with descriptions of three new genera. *Proceedings of the Entomological Society of
473 Washington*, 105:859–875.
- 474 Deans, A. R. (2002). *Papatuka alamunyiga* Deans, a new genus and species of apterous ensign wasp
475 (Hymenoptera: Evaniidae) from Kenya. *Zootaxa*, 95(1):1–8.
- 476 Deans, A. R. (2005). *Annotated catalog of the world's ensign wasp species (Hymenoptera: Evaniidae)*,
477 volume 34. American Entomological Institute.
- 478 Deans, A. R., Basibuyuk, H. H., Azar, D., and Nel, A. (2004). Descriptions of two new Early Cretaceous
479 (Hauterivian) ensign wasp genera (Hymenoptera: Evaniidae) from lebanese amber. *Cretaceous
480 Research*, 25(4):509–516.
- 481 Deans, A. R., Gillespie, J. J., and Yoder, M. J. (2006). An evaluation of ensign wasp classification
482 (Hymenoptera: Evaniidae) based on molecular data and insights from ribosomal RNA secondary
483 structure. *Systematic Entomology*, 31(3):517–528.
- 484 Deans, A. R. and Kawada, R. (2008). *Alobevania*, a new genus of neotropical ensign wasps (Hymenoptera:
485 Evaniidae), with three new species: integrating taxonomy with the World Wide Web. *Zootaxa*, 1787:28–
486 44.
- 487 Desjardins, C. A., Regier, J. C., and Mitter, C. (2007). Phylogeny of pteromalid parasitic wasps (Hy-
488 menoptera: Pteromalidae): initial evidence from four protein-coding nuclear genes. *Molecular
489 Phylogenetics and Evolution*, 45(2):454–469.
- 490 Downton, M. and Austin, A. D. (1994). Molecular phylogeny of the insect order Hymenoptera: Apocritan
491 relationships. *Proceedings of the National Academy of Sciences USA*, 91(21):9911–9915.
- 492 Downton, M. and Austin, A. D. (2001). Simultaneous analysis of 16S, 28S, COI and morphology in the
493 Hymenoptera: Apocrita—evolutionary transitions among parasitic wasps. *Biological Journal of the
494 Linnean Society*, 74(1):87–111.
- 495 Drummond, A. J., Nicholls, G. K., Rodrigo, A. G., and Solomon, W. (2002). Estimating mutation
496 parameters, population history and genealogy simultaneously from temporally spaced sequence data.
497 *Genetics*, 161(3):1307–1320.
- 498 Drummond, A. J. and Rambaut, A. (2007). BEAST: Bayesian evolutionary analysis by sampling trees.
499 *BMC evolutionary biology*, 7(1):214.
- 500 Drummond, A. J., Suchard, M. A., Xie, D., and Rambaut, A. (2012). Bayesian phylogenetics with
501 BEAUti and the BEAST 1.7. *Molecular biology and evolution*, 29(8):1969–1973.

- 502 Folmer, O., Black, M., Hoeh, W., Lutz, R., and Vrijenhoek, R. (1994). DNA primers for amplification of
503 mitochondrial cytochrome c oxidase subunit I from diverse metazoan invertebrates. *Molecular marine*
504 *biology and biotechnology*, 3(5):294–299.
- 505 Gillespie, J. J., Munro, J. B., Heraty, J. M., Yoder, M. J., Owen, A. K., and Carmichael, A. E. (2005a).
506 A secondary structural model of the 28S rRNA expansion segments D2 and D3 for chalcidoid wasps
507 (Hymenoptera: Chalcidoidea). *Molecular Biology and Evolution*, 22(7):1593–1608.
- 508 Gillespie, J. J., Yoder, M. J., and Wharton, R. A. (2005b). Predicted secondary structure for 28S and 18S
509 rRNA from Ichneumonoidea (Insecta: Hymenoptera: Apocrita): impact on sequence alignment and
510 phylogeny estimation. *Journal of Molecular Evolution*, 61(1):114–137.
- 511 Gonzalez, D. S. and Jordan, I. K. (2000). The α -mannosidases: phylogeny and adaptive diversification.
512 *Molecular Biology and Evolution*, 17(2):292–300.
- 513 Grimaldi, D. and Engel, M. S. (2005). *Evolution of the Insects*. Cambridge University Press.
- 514 Hall, T. A. (1999). BioEdit: a user-friendly biological sequence alignment editor and analysis program
515 for Windows 95/98/NT. In *Nucleic acids symposium series*, volume 41, pages 95–98. [London]:
516 Information Retrieval Ltd., c1979-c2000.
- 517 Hasegawa, M., Kishino, H., and Yano, T.-a. (1985). Dating of the human-ape splitting by a molecular
518 clock of mitochondrial dna. *Journal of molecular evolution*, 22(2):160–174.
- 519 Hedicke, H. (1939). Evaniidae. In Hedicke, H., editor, *Hymenopterum Catalogus Pars 9*. Dr. W. Junk,
520 Gravenhage.
- 521 Huben, M. (1995). Evaniidae. In Hanson, P. and Gauld, I., editors, *The Hymenoptera of Costa Rica*,
522 pages 195–199. Oxford University Press.
- 523 Jennings, J. T., Austin, A. D., and Stevens, N. B. (2004). *Hyptiogastrites electrinus* Cockerell, 1917,
524 from Myanmar (Burmese) amber: redescription and its placement within the Evanioidea (Insecta:
525 Hymenoptera). *Journal of Systematic Palaeontology*, 2(2):127–132.
- 526 Jennings, J. T. and Krogmann, L. (2009). A new species of *Pristaulacus* kieffer (Hymenoptera: Aulacidae)
527 from Baltic amber. *Insect Systematics & Evolution*, 40(2):201–207.
- 528 Jennings, J. T., Krogmann, L., and Mew, S. L. (2012). *Hyptia deansi* sp. nov., the first record of Evaniidae
529 (Hymenoptera) from Mexican amber. *Zootaxa*, 3349(1):63–68.
- 530 Jennings, J. T., Krogmann, L., and Priya, P. (2013). Happy birthday Willi Hennig!—*Hyptia hennigi* sp. nov.
531 (Hymenoptera: Evaniidae), a fossil ensign wasp from Eocene Baltic amber. *Zootaxa*, 3731:395–398.
- 532 Katoh, K. and Standley, D. M. (2013). MAFFT multiple sequence alignment software version 7:
533 improvements in performance and usability. *Molecular biology and evolution*, 30(4):772–780.
- 534 Kawada, R. (2011). Pictorial key for females of *Decevania* Huben (Hymenoptera, Evaniidae) and
535 description of a new species. *ZooKeys*, (116):59–84.
- 536 Kawada, R. and Azevedo, C. (2007). Taxonomic revision of the neotropical ensign wasp genus *Decevania*
537 (Hymenoptera: Evaniidae). *Zootaxa*, 1496(1):1–30.
- 538 Lanfear, R., Calcott, B., Ho, S. Y., and Guindon, S. (2012). PartitionFinder: combined selection of
539 partitioning schemes and substitution models for phylogenetic analyses. *Molecular biology and*
540 *evolution*, 29(6):1695–1701.
- 541 Legendre, F., Nel, A., Svenson, G. J., Robillard, T., Pellens, R., and Grandcolas, P. (2015). Phylogeny of
542 Dictyoptera: dating the origin of cockroaches, praying mantises and termites with molecular data and
543 controlled fossil evidence. *Plos ONE*, 10(7):e0130127.
- 544 Li, L., Rasnitsyn, A. P., Shih, C., Labandeira, C. C., Buffington, M., Li, D., and Ren, D. (2018). Phylogeny
545 of Evanioidea (Hymenoptera, Apocrita), with descriptions of new Mesozoic species from China and
546 Myanmar. *Systematic Entomology*, 43(4):810–842.
- 547 Li, W., Cowley, A., Uludag, M., Gur, T., McWilliam, H., Squizzato, S., Park, Y. M., Buso, N., and
548 Lopez, R. (2015). The embl-ebi bioinformatics web and programmatic tools framework. *Nucleic acids*
549 *research*, 43(W1):W580–W584.
- 550 Lohse, K., Sharanowski, B., Blaxter, M., Nicholls, J. A., and Stone, G. N. (2011). Developing EPIC
551 markers for chalcidoid hymenoptera from EST and genomic data. *Molecular ecology resources*,
552 11(3):521–529.
- 553 Lohse, K., Sharanowski, B., and Stone, G. N. (2010). Quantifying the Pleistocene history of the oak gall
554 parasitoid *Cecidostiba fungosa* using twenty intron loci. *Evolution*, 64(9):2664–2681.
- 555 Marchler-Bauer, A., Derbyshire, M. K., Gonzales, N. R., Lu, S., Chitsaz, F., Geer, L. Y., Geer, R. C., He,
556 J., Gwadz, M., Hurwitz, D. I., Lanczycki, C. J., Lu, F., Marchler, G. H., Song, J. S., Thanki, N., Wang,

- 557 Z., Yamashita, R. A., Zhang, D., Zheng, C., and Bryant, S. H. (2015). CDD: NCBI's conserved domain
558 database. *Nucleic Acids Research*, 43(D1):D222–D226.
- 559 Mardulyn, P. and Whitfield, J. B. (1999). Phylogenetic signal in the *coi*, 16s, and 28s genes for infer-
560 ring relationships among genera of Microgastrinae (Hymenoptera; Braconidae): evidence of a high
561 diversification rate in this group of parasitoids. *Molecular Phylogenetics and Evolution*, 12(3):282–294.
- 562 Mikó, I., Copeland, R. S., Balhoff, J. P., Yoder, M. J., and Deans, A. R. (2014). Folding wings like a
563 cockroach: a review of transverse wing folding ensign wasps (Hymenoptera: Evaniidae: *Afrevania* and
564 *Trissevania*). *PLoS ONE*, 9(5):e94056.
- 565 Miller, M. A., Pfeiffer, W., and Schwartz, T. (2010). Creating the CIPRES Science Gateway for inference
566 of large phylogenetic trees. In *Gateway Computing Environments Workshop (GCE), 2010*, pages 1–8.
567 IEEE.
- 568 Moulton, J. K. and Wiegmann, B. M. (2004). Evolution and phylogenetic utility of CAD (rudimen-
569 tary) among mesozoic-aged eremoneuran Diptera (Insecta). *Molecular phylogenetics and evolution*,
570 31(1):363–378.
- 571 Namin, H. H., Iranpour, M., and Sharanowski, B. J. (2014). Phylogenetics and molecular identification of
572 the *Ochlerotatus communis* complex (Diptera: Culicidae) using DNA barcoding and polymerase chain
573 reaction-restriction fragment length polymorphism. *The Canadian Entomologist*, 146(1):26–35.
- 574 Nel, A., Martínez-Delclòs, X., and Azar, D. (2002). A new ensign-fly from the Lower-Middle Miocene Do-
575 minican amber (Hymenoptera, Evaniidae). *Bulletin de la Société entomologique de France*, 107(3):217–
576 221.
- 577 Peters, R. S., Krogmann, L., Mayer, C., Donath, A., Gunkel, S., Meusemann, K., Kozlov, A., Podsiad-
578 lowski, L., Petersen, M., Lanfear, R., Diez, P. A., Heraty, J., Kjer, K. M., Klopstein, S., Meier, R.,
579 Polidori, C., Schmitt, T., Liu, S., Zhou, X., Wappler, T., Rust, J., Misof, B., and Niehuis, O. (2017).
580 Evolutionary history of the Hymenoptera. *Current Biology*, 27(7):1013–1018.
- 581 Peñalver, E., Ortega-Blanco, J., Nel, A., and Delclòs, X. (2010). Mesozoic Evaniidae (Insecta: Hy-
582 menoptera) in Spanish amber: Reanalysis of the phylogeny of the Evanioidea. *Acta Geologica Sinica*
583 (*English Edition*), 84(4):809–827.
- 584 Phillips, M. J., Delsuc, F., and Penny, D. (2004). Genome-scale phylogeny and the detection of systematic
585 biases. *Molecular biology and evolution*, 21(7):1455–1458.
- 586 Pitz, K. M., Dowling, A. P., Sharanowski, B. J., Boring, C. A., Seltmann, K. C., and Sharkey, M. J. (2007).
587 Phylogenetic relationships among the Braconidae (Hymenoptera: Ichneumonoidea): A reassessment of
588 Shi, Chen, and van Achterberg (2005). *Molecular Phylogenetics and Evolution*, 43(1):338–343.
- 589 Rambaut, A. (2012). FigTree v. 1. 4. *Molecular evolution, phylogenetics and epidemiology. Edinburgh,*
590 *UK: University of Edinburgh, Institute of Evolutionary Biology.*
- 591 Rambaut, A. and Drummond, A. (2009). Tracer v1.5. Available at [http://tree.bio.ed.ac.uk/
592 software/tracer/](http://tree.bio.ed.ac.uk/software/tracer/) Accessed 19 February 2018.
- 593 Rasnitsyn, A. P., Jarzembowski, E. A., and Ross, A. J. (1998). Wasps (Insecta: Vespida = Hymenoptera)
594 from the Purbeck and Wealden (Lower Cretaceous) of southern England and their biostratigraphical
595 and palaeoenvironmental significance. *Cretaceous Research*, 19(3-4):329–391.
- 596 Rodríguez-Ezpeleta, N., Brinkmann, H., Roure, B., Lartillot, N., Lang, B. F., and Philippe, H. (2007). De-
597 tecting and overcoming systematic errors in genome-scale phylogenies. *Systematic Biology*, 56(3):389–
598 399.
- 599 Ronquist, F., Klopstein, S., Vilhelmsen, L., Schulmeister, S., Murray, D. L., and Rasnitsyn, A. P. (2012a).
600 A total-evidence approach to dating with fossils, applied to the early radiation of the Hymenoptera.
601 *Systematic Biology*, 61(6):973–999.
- 602 Ronquist, F., Teslenko, M., Van Der Mark, P., Ayres, D. L., Darling, A., Höhna, S., Larget, B., Liu,
603 L., Suchard, M. A., and Huelsenbeck, J. P. (2012b). MrBayes 3.2: efficient Bayesian phylogenetic
604 inference and model choice across a large model space. *Systematic Biology*, 61(3):539–542.
- 605 Sawoniewicz, J. and Kupryjanowicz, J. (2003). *Evaniella eocenica* sp. nov. from the Baltic amber
606 (Hymenoptera: Evaniidae). *Acta Zoologica Cracoviensia*, 46(Suppl. - Fossil Insects):267–270.
- 607 Schulmeister, S., Wheeler, W. C., and Carpenter, J. M. (2002). Simultaneous analysis of the basal lineages
608 of Hymenoptera (Insecta) using sensitivity analysis. *Cladistics*, 18(5):455–484.
- 609 Sharanowski, B. J., Dowling, A. P., and Sharkey, M. J. (2011). Molecular phylogenetics of Braconidae
610 (Hymenoptera: Ichneumonoidea), based on multiple nuclear genes, and implications for classification.
611 *Systematic Entomology*, 36(3):549–572.

- 612 Sharanowski, B. J., Robbertse, B., Walker, J., Voss, S. R., Yoder, R., Spatafora, J., and Sharkey, M. J.
613 (2010). Expressed sequence tags reveal Proctotrupomorpha (minus Chalcidoidea) as sister to Aculeata
614 (Hymenoptera: Insecta). *Molecular phylogenetics and evolution*, 57(1):101–112.
- 615 Stadler, T. (2009). On incomplete sampling under birth-death models and connections to the sampling-
616 based coalescent. *Journal of theoretical biology*, 261(1):58–66.
- 617 Stamatakis, A. (2006). RAxML-VI-HPC: maximum likelihood-based phylogenetic analyses with thou-
618 sands of taxa and mixed models. *Bioinformatics*, 22(21):2688–2690.
- 619 Stamatakis, A. (2014). Raxml version 8: a tool for phylogenetic analysis and post-analysis of large
620 phylogenies. *Bioinformatics*, 30(9):1312–1313.
- 621 Swofford, D. L. (2002). PAUP* Phylogenetic analysis using parsimony (*and other methods). Version 4
622 beta. *Sunderland, MA: Sinauer Associates Inc, software*.
- 623 Tamura, K., Stecher, G., Peterson, D., Filipski, A., and Kumar, S. (2013). MEGA6: molecular evolutionary
624 genetics analysis version 6.0. *Molecular biology and evolution*, 30(12):2725–2729.
- 625 Timmermans, M., Roelofs, D., Mariën, J., and Van Straalen, N. (2008). Revealing pancrustacean
626 relationships: Phylogenetic analysis of ribosomal protein genes places Collembola (springtails) in
627 a monophyletic Hexapoda and reinforces the discrepancy between mitochondrial and nuclear DNA
628 markers. *BMC Evolutionary Biology*, 8(1):83.
- 629 Whitfield, J. B. (1997). Molecular and morphological data suggest a single origin of the polydnviruses
630 among braconid wasps. *Naturwissenschaften*, 84(11):502–507.
- 631 Winterton, S. and De Freitas, S. (2006). Molecular phylogeny of the green lacewings (Neuroptera:
632 Chrysopidae). *Austral Entomology*, 45(3):235–243.
- 633 Wool, I. G. (1979). The structure and function of eukaryotic ribosomes. *Annual review of biochemistry*,
634 48(1):719–754.
- 635 Zhang, C., Stadler, T., Klopstein, S., Heath, T., and Ronquist, F. (2015). Total-evidence dating under the
636 fossilized birth–death process. *Systematic Biology*, 65:228–249.

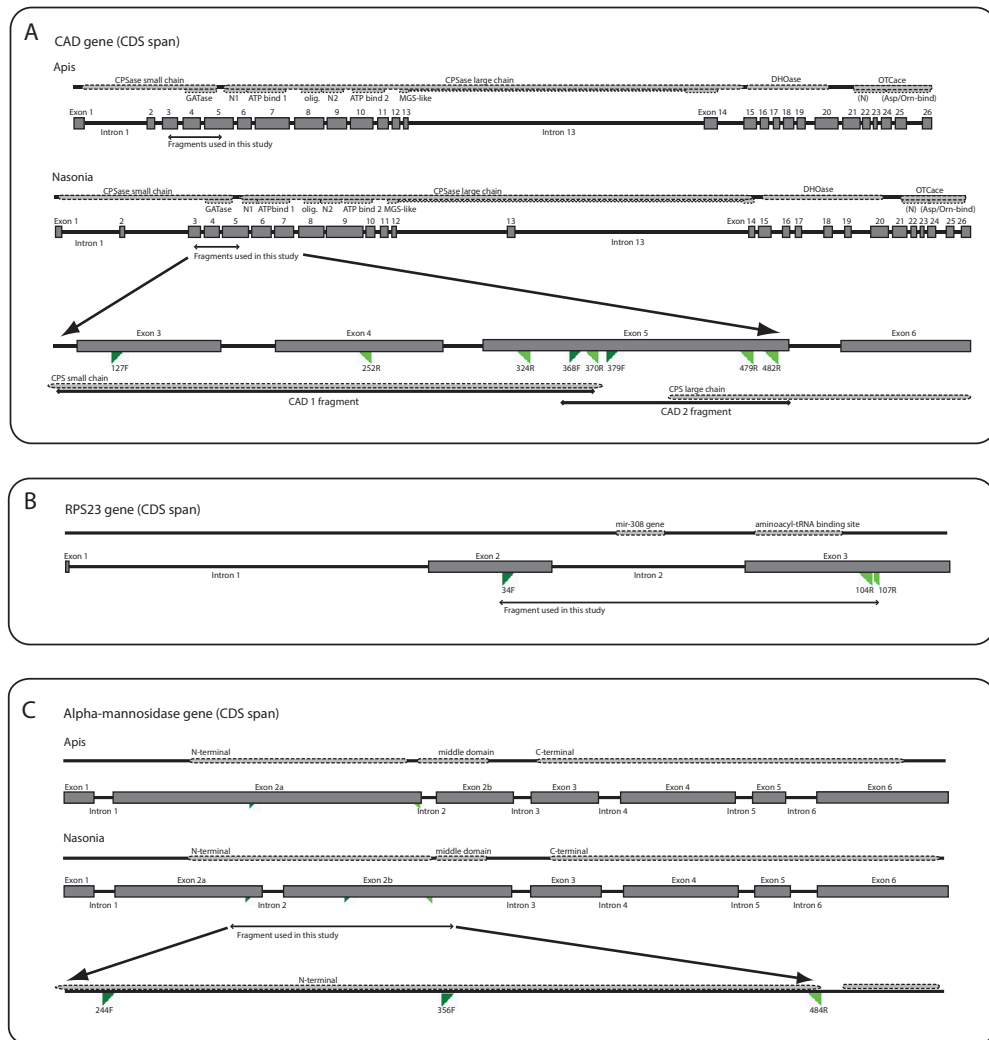


Figure 1. Diagrammatic gene maps for: **(A)** carbamoyl-phosphate synthetase-aspartate transcarbamoylase-dihydroorotase (*CAD*); **(B)** ribosomal protein S23 (*RPS23*); and **(C)** alpha-mannosidase II (*AM2*). Dotted lines mark protein domains and features. For *CAD* and *AM2*, *Apis* and *Nasonia* gene diagrams are shown individually as references due to substantial differences in exon locations. The bottom diagram in each gene map depicts the regions amplified in this study. In *CAD*, intron 13 in *Nasonia* has been scaled down due to an incomplete sequence in the GenBank entry. Primers are named according to the amino acid position in the *Apis mellifera* protein. Forward primers are in dark green and reverse primers in light green. See Table S2 for primer combinations. Abbreviations: *CPS*, carbamoyl-phosphate synthase; *GAT*, glutamine aminotransferase; *DHO*, dihydroorotase; *MGS*, methylglyoxal-like; *OTC*, ornithine carbamoyltransferase; *SNI*, N-terminal of subunit 1 in *CPS* large chain; *N2*, N-terminal of subunit 2 in *CPS* large chain; olig., oligomerization domain.



Figure 2. Bayesian analysis of phylogenetic relationships among Evaniidae. The outgroups were removed and placed above the ingroup tree for better visualization (the scale has been retained). Posterior probabilities are listed beside each clade.

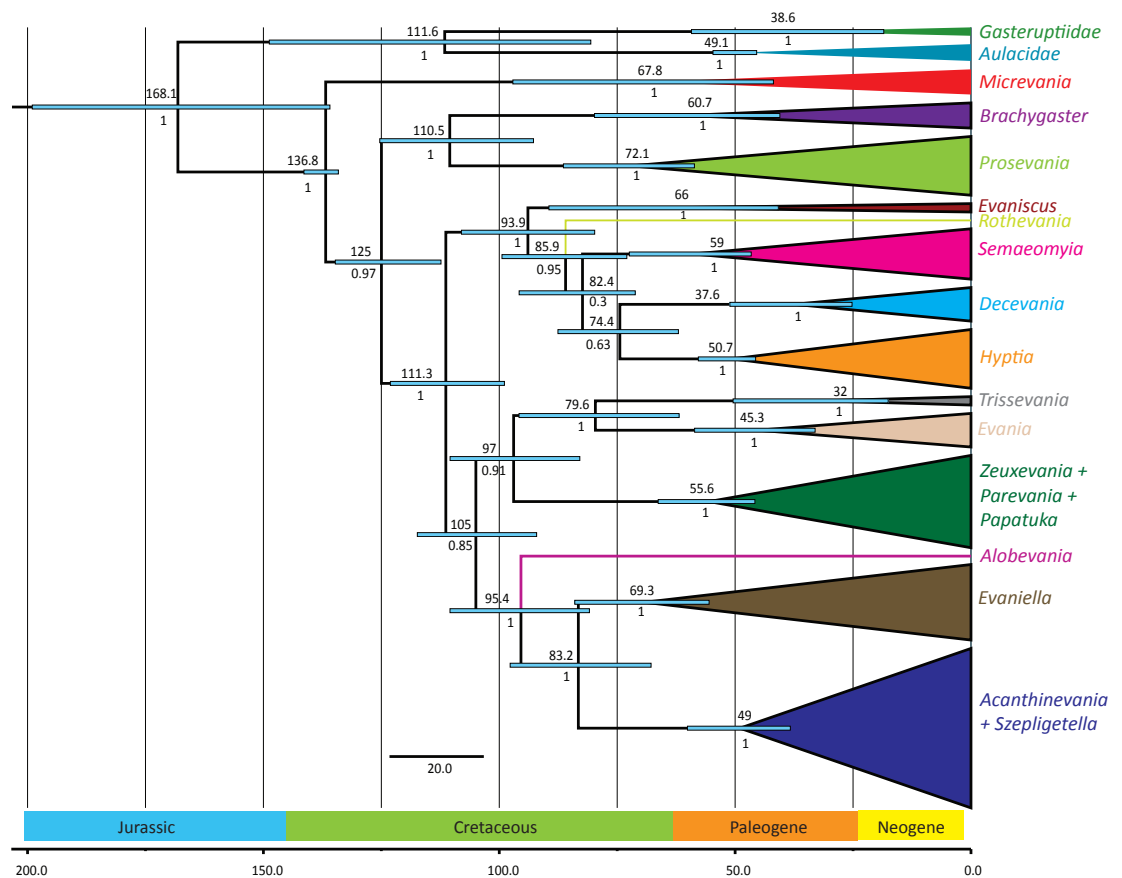


Figure 3. Simplified chronogram showing estimated divergence times for Evaniidae with six fossil calibrations and maximum clade ages under a lognormal distribution. Monophyletic genera have been collapsed for better visualization of the divergence estimations of the major clades. The blue bars indicate the 95% highest posterior density interval (HDI, also listed in Table 1). The scale is in millions of years. Mean age is listed above each clade and posterior probabilities are listed below .